XIV International Conference on Computational Plasticity. Fundamentals and Applications
COMPLAS 2017
E. Oñate, D.R.J. Owen, D. Peric and M. Chiumenti (Eds)

FLEXIBILITY OF APPROXIMATION IN PIES APPLIED FOR SOLVING ELASTOPLASTIC BOUNDARY PROBLEMS

AGNIESZKA BOŁTUĆ

Faculty of Mathematics and Informatics
University of Bialystok
K. Ciołkowskiego 1M, 15-245 Białystok, Poland
e-mail: aboltuc@ii.uwb.edu.pl

Key words: Approximation, Local vs. global, Elastoplastic, Boundary problems, PIES.

Abstract. The paper presents the flexibility of approximation in PIES applied for solving elastoplastic boundary value problems. Three various approaches to approximation of plastic strains have been tested. The first one bases on the globally applied Lagrange polynomial. The two remaining are local: inverse distance weighting (IDW) method and approximation in different zones by locally applied Lagrange polynomials. Some examples are solved and results obtained are compared with analytical solutions. Conclusions on the effectiveness of presented approaches have been drawn.

1 INTRODUCTION

The main issue of solving boundary value problems by the finite element method (FEM) [1,2] and the boundary element method (BEM) [3,4] is discretization. The approach called parametric integral equation system (PIES)[5] has been developed as an alternative to mentioned methods. It is characterized by analytical incorporation of curves and surfaces into the integral equation, which results in separation of approximations: the shape from the solutions. It means that more effective methods for both approximations can be applied. PIES with mentioned advantages has been applied for solving various problems e.g. acoustic [6], elastic [7,8] or lately elasto-plastic [9].

Solving elasto-plastic problems, in PIES like in BEM, only the plastic region has to be modelled. It is defined globally using surface patches known from computer graphics [10,11]. In most cases only single surface is enough. For this reason also approximation of plastic strains is done globally using various polynomials (e.g. the Lagrange polynomial). Such an approach has pros and cons. Advantageous is simple global integration with a bit more number of weights in the quadrature and without the necessity of calculating integrals over small regular areas and summing them. The second benefit is flexibility of obtaining plastic strains at any point of the considered domain, because it is done continuously using only one formula. On the other hand, it is known that plastic strains occur locally. Even if the defined surface covers only the estimated plastic zone, a part of it is characterized by a zero plastic deformations. Using global approximation every calculated value is more or less affected by values from all interpolation nodes. It means that there is no possibility to obtain exactly zero at nodes which are not plastic, but only a value that oscillates around zero. The accuracy of

the results obtained using the global approach depends on the number of interpolation nodes. The more interpolation nodes with zero plastic strains, the more accurate results in the vicinity of zero can be obtained between them. When a lot of nodes have to be taken in order to guarantee appropriate accuracy, a local approximation should be considered. However, in order not to lose the main advantage of PIES, local approximation cannot be associated with shape discretization.

The main aim of this paper is to develop and test various methods of local approximation without the necessity of dividing the domain into elements or cells. At the beginning, approximation is separated into two or more zones depending on the distribution of plastic strains. This division is done only on the interpolation nodes level. However, there are also problems that require totally local approach around the considered node only. The inverse distance weighting (IDW) method is an example of the method using this approach and it can be easily adapted to PIES. Some examples are solved using both approaches. The results obtained confirm the effectiveness of proposed methods of approximation.

2 PIES AND THE INTEGRAL IDENTITY FOR STRESSES

The parametric integral equation system (PIES) in the initial-strain approach was derived and presented in [9]. The resulting form of PIES is given by

$$0.5\dot{\boldsymbol{u}}_l(\bar{s}) = \sum_{j=1}^{n} \int_{s_{j-1}}^{s_j} \left\{ \overline{\boldsymbol{U}}_{lj}^{\,*}(\bar{s},s)\dot{\boldsymbol{p}}_j(s) - \overline{\boldsymbol{P}}_{lj}^{\,*}(\bar{s},s)\dot{\boldsymbol{u}}_j(s) \right\} J_j(s)ds + \int_{v_{d-1}}^{v_d}\int_{w_{d-1}}^{w_d} \overline{\boldsymbol{\sigma}}_l^{\,*}(\bar{s},v,w)\dot{\boldsymbol{\varepsilon}}^p(v,w)J_d(v,w)dvdw, \tag{1}$$

where $s_{l-1} \le \bar{s} \le s_l$, $s_{j-1} \le s \le s_j$, $v_{d-1} \le v \le v_d, w_{d-1} \le w \le w_d$. Variable n is the number of segments that built a boundary, while m is the number of surfaces that built a domain, therefore $l = 1,2,.....n$ and $d = 1,2,....., m$.

As is stated in the introduction, boundary segments in PIES can be defined by any curves $\boldsymbol{\Gamma}_j(s)$ (e.g. Bézier, Hermite, B-spline or NURBS curves) and s_{l-1} and s_{j-1} correspond to the beginning of lth and jth segments, while s_l and s_j to the end of these segments. Consequently, a domain in PIES can be defined by surface patches (e.g. Bézier surface patches) and $v_{d-1}, v_d, w_{d-1}, w_d$ are respectively the beginning and the end of the domain of dth surface. For the sake of simplicity, it should be remembered that the domain of the surface is a unit square $[0,1]\times[0,1]$. Mapping integral intervals require introduction of scaling factors (Jacobians), which can be presented as follows

$$J_j(s) = \left[\left(\frac{\partial \Gamma_j^{(1)}(s)}{\partial s} \right)^2 + \left(\frac{\partial \Gamma_j^{(2)}(s)}{\partial s} \right)^2 \right]^{0.5}, \qquad \text{for a boundary segments,} \tag{2}$$

and

$$J_d(v,w) = [A_1^2(v,w) + A_2^2(v,w) + A_3^2(v,w)]^{0.5}, \qquad \text{for a domain,} \tag{3}$$

where functions $A_1(v,w), A_2(v,w), A_3(v,w)$ represent the combination of the partial derivatives of mathematical functions that describe surfaces [10,11].

Functions $\dot{\boldsymbol{p}}_j(s), \dot{\boldsymbol{u}}_j(s)$ from (1) are parametric boundary functions defined or searched on each segment of the boundary, while $\dot{\boldsymbol{\varepsilon}}^p(v,w)$ are plastic strains. Since PIES is solved using the collocation method, $\bar{s}$ stands for a collocation point.

Equation (1) contains three kernels. The first kernel $\overline{\boldsymbol{U}}^*_{lj}(\bar{s},s)$ for the plane strain case is presented in the following matrix form [9]

$$\overline{\boldsymbol{U}}^*_{lj}(\bar{s},s) = -\frac{1}{8\pi(1-\nu)\mu}\begin{bmatrix} (3-4\nu)\ln(\eta)-\dfrac{\eta_1^2}{\eta^2} & -\dfrac{\eta_1\eta_2}{\eta^2} \\ -\dfrac{\eta_1\eta_2}{\eta^2} & (3-4\nu)\ln(\eta)-\dfrac{\eta_2^2}{\eta^2} \end{bmatrix}, \qquad l,j=1,2,.....n, \tag{4}$$

where $\eta=[\eta_1^2+\eta_2^2]^{0.5}$, $\eta_1=\Gamma_j^{(1)}(s)-\Gamma_l^{(1)}(\bar{s})$, $\eta_2=\Gamma_j^{(2)}(s)-\Gamma_l^{(2)}(\bar{s})$, while ν is Poisson's ratio and μ is a shear modulus.

The next kernel $\overline{\boldsymbol{P}}^*_{lj}(\bar{s},s)$ in (1) can be presented by the expression [9]

$$\overline{\boldsymbol{P}}^*_{lj}(\bar{s},s) = -\frac{1}{4\pi(1-\nu)\eta}\begin{bmatrix} P_{11} & P_{12} \\ P_{21} & P_{22} \end{bmatrix}, \quad l,j=1,2,.....n, \tag{5}$$

where

$$P_{11}=\left\{(1-2\nu)+2\frac{\eta_1^2}{\eta^2}\right\}\frac{\partial\eta}{\partial n}, \quad P_{12}=\left\{2\frac{\eta_1\eta_2}{\eta^2}\frac{\partial\eta}{\partial n}-(1-2\nu)\left[\frac{\eta_1}{\eta}n_2(\mathrm{s})+\frac{\eta_2}{\eta}n_1(\mathrm{s})\right]\right\},$$

$$P_{21}=\left\{2\frac{\eta_2\eta_1}{\eta^2}\frac{\partial\eta}{\partial n}-(1-2\nu)\left[\frac{\eta_2}{\eta}n_1(\mathrm{s})+\frac{\eta_1}{\eta}n_2(\mathrm{s})\right]\right\}, \quad P_{22}=\left\{(1-2\nu)+2\frac{\eta_2^2}{\eta^2}\right\}\frac{\partial\eta}{\partial n},$$

$$\frac{\partial\eta}{\partial n}=\frac{\partial\eta_1}{\partial\eta}n_1(\mathrm{s})+\frac{\partial\eta_2}{\partial\eta}n_2(\mathrm{s}),$$

and $n_1(s)$ and $n_2(s)$ are the direction cosines of the external normal to j*th* segment of the boundary.

Both kernels (4) and (5) take into account (in their mathematical formalism) the shape of the boundary defined by any parametric curves $\boldsymbol{\Gamma}(s)$. The shape of the domain defined by any parametric surfaces $\boldsymbol{B}(v,w)$ is integrated into the integrand $\overline{\boldsymbol{\sigma}}^*_l(\bar{s},v,w)$ from (1). For the plane strain case that function can be presented as follows [9]

$$\overline{\sigma}^*_l(\bar{s},v,w) = -\frac{1}{4\pi(1-\nu)\overline{\eta}}\begin{bmatrix} (1-2\nu)\dfrac{\overline{\eta}_1}{\overline{\eta}}+2\dfrac{\overline{\eta}_1^3}{\overline{\eta}^3}-2\nu\dfrac{\overline{\eta}_1}{\overline{\eta}} & (1-2\nu)\dfrac{\overline{\eta}_2}{\overline{\eta}}+2\dfrac{\overline{\eta}_1^2\overline{\eta}_2}{\overline{\eta}^3} \\ -(1-2\nu)\dfrac{\overline{\eta}_2}{\overline{\eta}}+2\dfrac{\overline{\eta}_1^2\overline{\eta}_2}{\overline{\eta}^3}-2\nu\dfrac{\overline{\eta}_2}{\overline{\eta}} & (1-2\nu)\dfrac{\overline{\eta}_1}{\overline{\eta}}+2\dfrac{\overline{\eta}_2^2\overline{\eta}_1}{\overline{\eta}^3} \\ (1-2\nu)\dfrac{\overline{\eta}_2}{\overline{\eta}}+2\dfrac{\overline{\eta}_2\overline{\eta}_1^2}{\overline{\eta}^3} & -(1-2\nu)\dfrac{\overline{\eta}_1}{\overline{\eta}}+2\dfrac{\overline{\eta}_2^2\overline{\eta}_1}{\overline{\eta}^3}-2\nu\dfrac{\overline{\eta}_1}{\overline{\eta}} \\ (1-2\nu)\dfrac{\overline{\eta}_1}{\overline{\eta}}+2\dfrac{\overline{\eta}_2^2\overline{\eta}_1}{\overline{\eta}^3} & (1-2\nu)\dfrac{\overline{\eta}_2}{\overline{\eta}}+2\dfrac{\overline{\eta}_2^3}{\overline{\eta}^3}-2\nu\dfrac{\overline{\eta}_2}{\overline{\eta}} \end{bmatrix}^{\mathrm{T}}, \tag{6}$$

where $\overline{\eta}=[\overline{\eta}_1^2+\overline{\eta}_2^2]^{0.5}$, $\overline{\eta}_1=B^{(1)}(v,w)-\Gamma_l^{(1)}(\bar{s})$ and $\overline{\eta}_2=B^{(2)}(v,w)-\Gamma_l^{(2)}(\bar{s})$.

Formula (1) allows obtaining displacements and forces on the boundary. To determine other quantities within the domain the integral identity is required. In order to calculate stresses the following expression has to be used

$$\dot{\boldsymbol{\sigma}}(\boldsymbol{x}) = \sum_{j=1}^{n} \int_{s_{j-1}}^{s_j} \{\hat{\hat{\boldsymbol{D}}}_j^*(\boldsymbol{x},s)\dot{\boldsymbol{p}}_j(s) - \hat{\hat{\boldsymbol{S}}}_j^*(\boldsymbol{x},s)\dot{\boldsymbol{u}}_j(s)\} J_j(s)ds + \\ + \int_{v_{d-1}}^{v_d} \int_{w_{d-1}}^{w_d} \hat{\hat{\boldsymbol{\Sigma}}}^*(\boldsymbol{x},v,w)\dot{\boldsymbol{\varepsilon}}^p(v,w) J_d(v,w)dvdw + \hat{\hat{\boldsymbol{f}}}\dot{\boldsymbol{\varepsilon}}^p(\boldsymbol{x}) \tag{7}$$

Kernels $\hat{\hat{\boldsymbol{D}}}_j^*(\boldsymbol{x},s)$, $\hat{\hat{\boldsymbol{S}}}_j^*(\boldsymbol{x},s)$, $\hat{\hat{\boldsymbol{\Sigma}}}^*(\boldsymbol{x},v,w)$ and also a free term are given in explicit form in [9].

3 DEFINING THE DOMAIN

As is stated in section 2, the domain in the proposed method is modeled globally using surface patches [10,11]. Till now only Bézier surfaces were applied, but the approach gives flexibility in choosing the type of patch. In PIES, like in BEM, only the yield region is defined, because the domain integrals are zero elsewhere. In order to show the way of modeling in PIES two different shapes are considered. The first domain is polygonal, the second curvilinear and both of them are presented in [12]. Figure 1 and 2 present them discretized in BEM and defined in PIES. White circles ○ represent nodes required to define the boundary, while black ● are those which are necessary for the yield region modeling.

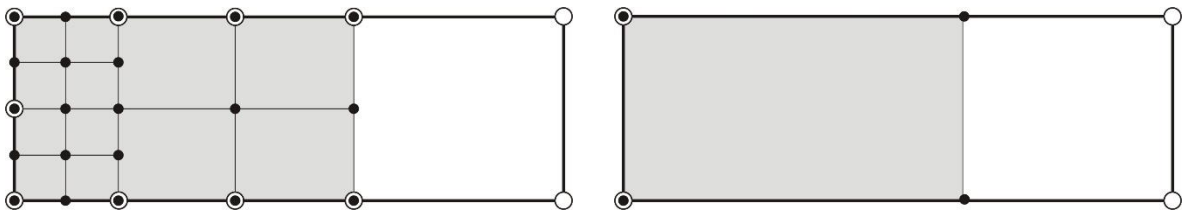

a) b)

Figure 1: Modeling a cantilever beam in: a) BEM, b) PIES

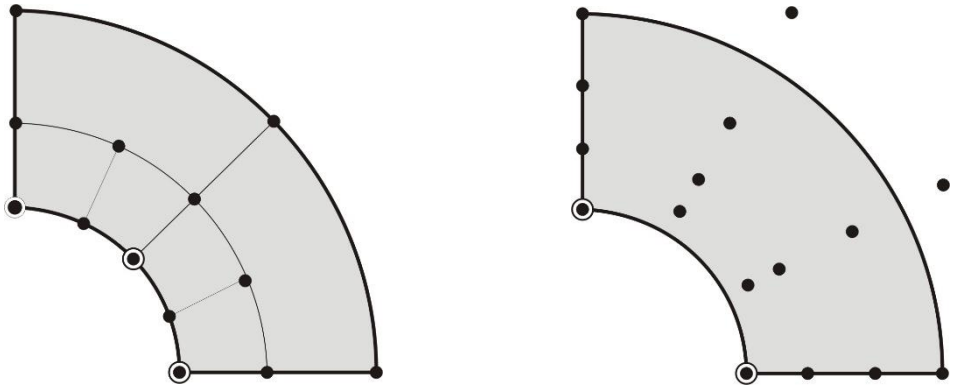

a) b)

Figure 2: Modeling a circular hole in an infinite domain in: a) BEM, b) PIES

As can be seen in Fig. 1a and 2a, the discretization requires division of yield region into cells. They model the geometry, but also their number and type are responsible for the accuracy of obtained solutions. Therefore, even if the shape can be modeled using smaller number of cells, sometimes (or even very often) they have to be multiplied in order to maintain satisfactory level of results. Thus, the yield region in the cantilever beam (Fig. 1a) in BEM is defined by 12 linear cells and 21 nodes, while in fact it can be modeled using only one bilinear surface and 4 corner points (Fig. 1b). The same situation is when the curved shape is defined. In BEM there is the necessity of applying 6 linear cells (Fig. 2a), while PIES requires only one bicubic surface (Fig. 2b).

Concluding, the number of data required for modeling the domain in PIES depends only on the complexity of a shape. The accuracy of approximation is guaranteed by the number of expressions in approximation series presented in the next section. Proposed method solves also another complication occurring in BEM. The extent of the yield region is not known a priori, therefore very often generous proportion of it are assumed initially. For this reason the greater number of cells has to be defined. In PIES that problem does not exists, because as it is presented in Fig.1b using the same number of nodes even entire domain can be modeled as an initial yield region. Thus, it is more effective to assume quite large proportions than performing pilot studies.

4 APPROXIMATION OF PLASTIC STRAINS

4.1 Global approximation using Lagrange polynomials

As is mentioned in section 3, approximations of the shape and solutions in PIES are performed independently. Therefore, the domain can be modeled globally using only minimal number of data needed for accurate definition of the shape. A consequence of the global modeling of the plastic zone is the possibility of global approximation of plastic strains. For this purpose any 2D method can be used. Till now I have applied the approximation series with Chebyshev basis functions and Lagrange polynomials. The first approach has one disadvantage i.e. it requires solving of the system of equations. This feature can be unfavorable especially when the system is ill-conditioned. The second way is not characterized by this defect, and therefore is more efficient.

Using the Lagrange polynomials the plastic strains $\dot{\boldsymbol{\varepsilon}}^p(\boldsymbol{x})$ can be approximated by the following approximation series

$$\dot{\boldsymbol{\varepsilon}}^p(\boldsymbol{x}) = \sum_{r=0}^{R_1-1}\sum_{w=0}^{R_2-1} \dot{\boldsymbol{\varepsilon}}^{p,rw}(\boldsymbol{x}) L_{rw}(\boldsymbol{x}) \,, \tag{8}$$

where

$$L_{rw}(\boldsymbol{x}) = L_r(x_1) L_w(x_2),$$

$$L_r(x_1) = \prod_{o=0,o\neq r}^{R_1-1} \frac{x_1 - x_{1o}}{x_{1r} - x_{1o}}, \quad L_w(x_2) = \prod_{o=0,o\neq w}^{R_2-1} \frac{x_2 - x_{2o}}{x_{2w} - x_{2o}},$$

and $N = R_1 \cdot R_2$ is the given number of interpolation nodes, while $\dot{\boldsymbol{\varepsilon}}^{p,rw}(\boldsymbol{x})$ is the value of plastic strain at the node (x_{1r}, x_{2w}).

One of the most crucial elements of the approximation is arrangement of interpolation nodes. Taking into account the domain of approximation – a unit square – it is very easy to distribute nodes in any order. Some orders that were previously successfully used are:

uniform and at zeros of Chebyshev polynomial. Using the first method and quite large number of interpolation nodes Runge's phenomenon may occur. Therefore, the most efficient and safe is the second proposition. Nodes placed in the unit square have to be transformed into the actual domain in order to obtain values of plastic strains for approximation. This is also simple, because each surface is described by some formulas, which translate coordinates from the parametric domain of the surface to Cartesian coordinate system.

After substituting formula (8) into (1) and using approximating series for the boundary functions (presented in [9]) we obtain approximating form of PIES for elastoplastic problems

$$0.5\dot{\boldsymbol{u}}_l(\bar{s}) = \sum_{j=1}^{n}\sum_{k=0}^{M-1}\left\{\dot{\boldsymbol{p}}_j^{(k)}\int_{s_{j-1}}^{s_j}\overline{\boldsymbol{U}}_{lj}^{\,*}(\bar{s},s) - \dot{\boldsymbol{u}}_j^{(k)}\int_{s_{j-1}}^{s_j}\overline{\boldsymbol{P}}_{lj}^{\,*}(\bar{s},s)\right\} t_j^{(k)}(s)J_j(s)ds + \\ + \int_{v_{d-1}}^{v_d}\int_{w_{d-1}}^{w_d}\overline{\boldsymbol{\sigma}}_l^{*}(\bar{s},v,w)J_d(v,w)\sum_{r=0}^{R_1-1}\sum_{w=0}^{R_2-1}\dot{\boldsymbol{\varepsilon}}^{p,rw}(\boldsymbol{x})L_{rw}(v,w)dvdw. \tag{9}$$

As can be seen in (9), the domain integral is calculated on the basis of values returned by the formula (8), which is used globally (one formula for the whole surface). The advantage of the approach is that we have only one polynomial by which plastic strains at arbitrary points of the plastic region can be obtained. On the other hand, this approach may not reflect the local character of strains. It means that every point which does not yield has plastic strains only around zero, but not exactly zero. It comes from the fact, that all interpolation nodes have influence on searched values. Therefore, maybe it is reasonable to separate approximation into two or more zones depending on the distribution of plastic strains.

4.2 Local approximation

4.2.1 Different Lagrange polynomials in different zones

In PURC separation of approximations is very easy, because approximation of the domain and approximation of the plastic strains are independent. Thus, the shape still is modeled by the surface, interpolation nodes are generated in its domain (the unit square) and approximation is done by manipulating these nodes. Such an approach allows to separate two sets of nodes and for approximation of strains to use two approximation polynomials. Most expected division is the one, which separates zone with nonzero plastic strains from that where they are zero. The example of such a division for the Lame problem is presented in Fig. 3. The analytical solution for this problem is known, therefore the boundary of the division is drawn as the boundary between elastic and plastic regions.

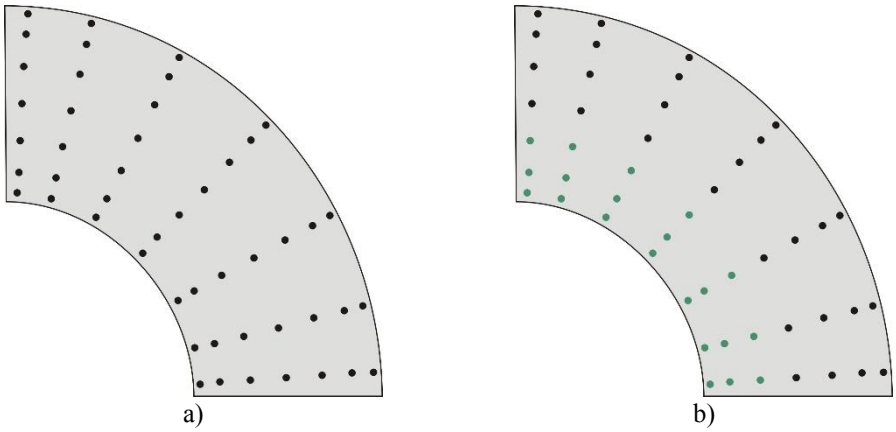

Figure 3: a) An arrangement of interpolation nodes, b) split into two sets of nodes

Each point for which plastic strains are required has to be assigned to one of the approximation zones and depending on the choice its value should be approximated with the appropriate polynomial. Zone boundaries can be arbitrarily chosen, however, it seems intuitively that it should divide the domain evenly between the extreme nodes of the designated sets of nodes. Dividing a plastic region into zones is straightforward in the proposed method, since approximation takes place in the unit square, which is a domain of the surface. An example of division into zones of influence of individual approximation polynomials is shown in Fig. 4.

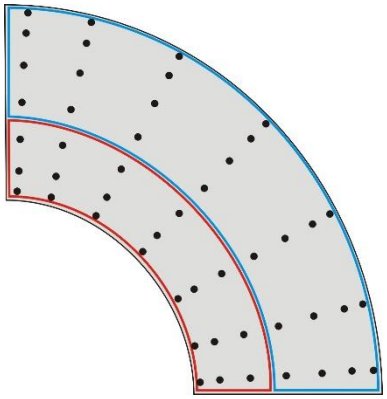

Figure 4: Two zones for which are used different approximation series

As can be seen in Fig. 4, for all points included in the red and blue zones different polynomials have to be used.

The PIES approximation form described by (9) has to be modified, and the last term of the equation

$$\int_{v_{d-1}}^{v_d}\int_{w_{d-1}}^{w_d} \overline{\boldsymbol{\sigma}}_l^*(\bar{s},v,w)J_d(v,w)\sum_{r=0}^{R_1-1}\sum_{w=0}^{R_2-1}\dot{\boldsymbol{\varepsilon}}^{p,rw}(\boldsymbol{x})L_{rw}(v,w)dvdw,$$

is replaced by

$$\int_{v_{d-1}}^{v_d}\int_{w_{d-1}}^{w_d} \overline{\boldsymbol{\sigma}}_l^*(\bar{s},v,w)J_d(v,w)\sum_{r=0}^{T_1-1}\sum_{w=0}^{T_2-1}\dot{\boldsymbol{\varepsilon}}^{p,rw}(\boldsymbol{x})L_{rw}(v,w)dvdw, \tag{10}$$

where T_1, T_2 are numbers of interpolation points assigned to the corresponding Lagrange polynomial. Considering the example presented in Fig.4 the first polynomial is characterized by $T_1 = 3$ and $T_2 = 7$, while the second by $T_1 = 4$ and $T_2 = 7$. Which of the polynomials will be used to approximate $\dot{\boldsymbol{\varepsilon}}^p(v,w)$ in (10) depends on the location of point $\boldsymbol{x}$.

Similar modifications should also be made to the last element of the approximation form of the integral identity for stress (7). The situation is a little more complicated here, because the integral over the domain is strongly singular. In [9], the algorithm described in [13] was used for its determination. It consists in transforming the singular integral into two

$$\begin{aligned}&\int_{v_{d-1}}^{v_d}\int_{w_{d-1}}^{w_d} \hat{\overline{\boldsymbol{\Sigma}}}^*(\boldsymbol{x},v,w)\dot{\boldsymbol{\varepsilon}}^p(v,w)J_d(v,w)dvdw= \\ &\int_{v_{d-1}}^{v_d}\int_{w_{d-1}}^{w_d} \hat{\overline{\boldsymbol{\Sigma}}}^*(\boldsymbol{x},v,w)[\dot{\boldsymbol{\varepsilon}}^p(v,w)-\dot{\boldsymbol{\varepsilon}}^p(\boldsymbol{x})]J_d(v,w)dvdw+\dot{\boldsymbol{\varepsilon}}^p(\boldsymbol{x})\int_{v_{d-1}}^{v_d}\int_{w_{d-1}}^{w_d} \hat{\overline{\boldsymbol{\Sigma}}}^*(\boldsymbol{x},v,w)J_d(v,w)dvdw\end{aligned} \tag{11}$$

The first integral is weakly singular and can be evaluated by subdivision technique, while the second has been transformed into a boundary integral with no singularity. In both integrals it is necessary to use the approximation series (8) twice to calculate the plastic strains at the point $\boldsymbol{x}$ and for all points (v,w). And again like in (10), one should use polynomials that correspond to positions of both points.

The advantage of the proposed strategy is that the number of interpolation nodes in a polynomial can be quite effectively controlled. For example, if one of the polynomials is used to approximate strains where most of them are zero, it can be built with smaller number of nodes. An example of the strategy is presented in Fig. 5.

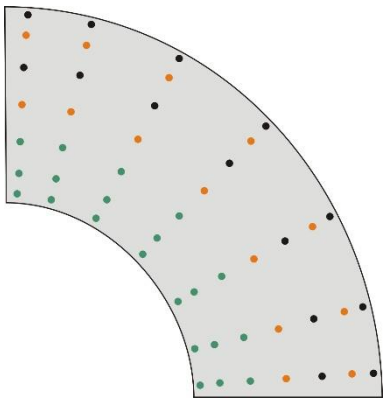

Figure 5. Interpolation nodes used in two approximation series

As shown in Fig. 5, green nodes have been used in one of the polynomials, while in the second is considered only every second row of nodes marked by orange.

The strategy described in this section, despite being based on globally generated nodes and a globally modeled plastic region, is zonally local. However, there are issues that require approximation to be completely local to the selected point. There are many local

approximation algorithms, most of which can be easily adapted to PIES. One of the simplest examples is the inverse distance weighting (IDW) method.

4.2.2 Inverse distance weighting

Inverse distance weighting (IDW), also known as the Shepard method, is used for interpolation with an irregularly-spaced interpolation nodes [14]. Unknown values are calculated with a weighted average of the values available at the known nodes. A general form of finding an interpolated value $\dot{\boldsymbol{\varepsilon}}^p(\boldsymbol{x})$ at a given point $\boldsymbol{x}$ based on plastic strains $\dot{\boldsymbol{\varepsilon}}^p(\boldsymbol{x}_r)$ ($r = 0,1,...R$) at R interpolation points using IDW is

$$\dot{\boldsymbol{\varepsilon}}^p(\boldsymbol{x}) = \begin{cases} \dfrac{\sum_{r=0}^{R} \omega_r(\boldsymbol{x}) \dot{\boldsymbol{\varepsilon}}^p(\boldsymbol{x}_r)}{\sum_{r=0}^{R} \omega_r(\boldsymbol{x})}, & if\ d(\boldsymbol{x},\boldsymbol{x}_r) \neq 0\ \ for\ all\ r \\ \dot{\boldsymbol{\varepsilon}}^p(\boldsymbol{x}_r), & if\ d(\boldsymbol{x},\boldsymbol{x}_r) = 0\ \ for\ some\ r \end{cases}, \tag{12}$$

where

$$\omega_r(\boldsymbol{x}) = \frac{1}{d(\boldsymbol{x},\boldsymbol{x}_r)^p}, \tag{13}$$

is a simple IDW weighting function, d is a given distance from the known point $\boldsymbol{x}_r$ to the unknown point $\boldsymbol{x}$ and p is a positive real number, called the power parameter.

The main idea of IDW is that things that are close to one another are more alike than those that are farther apart. To predict a value for any unmeasured location, IDW uses the measured values surrounding the prediction location (from so-called neighborhood of influence). It is known that using such an approach the accuracy depends on the arrangement of interpolation nodes and the way of determination of the mentioned neighborhood. In the simplest case the neighborhood of influence can be specified using maximal distance from point of interest and it is just a spatially fixed shape e.g. circle. Selection of interpolation nodes could be much more complex, but also more effective especially in cases with highly nonregularly distributed nodes [15].

In the paper, the simplest method of determining the neighborhood of influence is used. Fig. 6 presents nodes used for approximation of plastic strain at point $\boldsymbol{x}$.

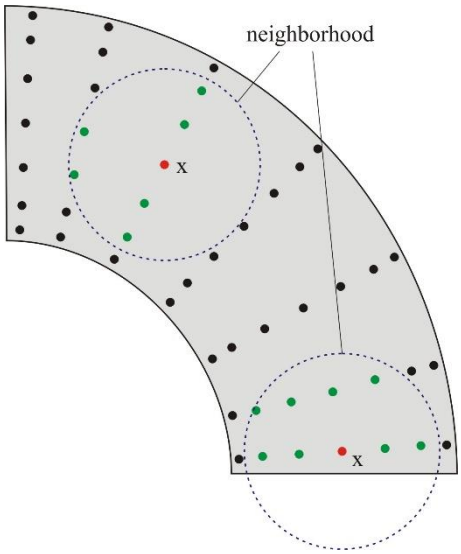

Figure 6: Neighborhood determines nodes for approximation at points $\boldsymbol{x}$

Another factor affecting the accuracy of the approximation in IDW is the power parameter p. Greater values of p assign greater influence to values closest to the approximated point.

5 RESULTS

5.1 Different Lagrange polynomials in different zones

The first example concerns a thick-walled cylinder subjected to internal pressure under plain strain conditions. The radius of inner face is $a = 100$, while outer face is $b = 200$. The whole domain is defined by one bicubic Bézier surface. The Von-Mises yield criterion with perfect plasticity and the following material constants $\sigma_Y = 30 MPa$, $E = 21000 MPa$, $v = 0.3$ are assumed.

Initially, the problem was solved using global approach with 25 and 36 interpolation nodes placed at roots of Chebyshev polynomials. For those two cases, radial and circumferential stress distribution for a specific ($p = 20.9 MPa$) internal pressure were calculated. Values obtained at 100 internal points are used to calculate a norm L_2

$$\|e\| = \frac{1}{\left|\overline{\sigma}_r^w\right|_{\max}} \sqrt{\frac{1}{100} \sum_{w=1}^{100} (\sigma_r^w - \overline{\sigma}_r^w)^2} \times 100\% , \tag{14}$$

where σ_r^w represents radial stresses obtained by PIES at 100 interior points, while $\overline{\sigma}_r^w$ are exact solutions [16]. Values of norm for two assumed numbers of interpolation nodes are presented in Table 1.

Table 1: Norms for radial and circumferential stress distribution – global approximation

	25	**36**
$\|e\|_{\sigma_r}$	0.4432	0.1923
$\|e\|_{\sigma_q}$	2.4478	1.4653

As can be seen in Table 1 value of norm is smaller for higher number of interpolation nodes, but it still can be better (especially for σ_q). For this reason the first technique described in section 4.2.1 is applied. Three different cases are considered: two of them with 36 and one with 25 interpolation nodes. Figure 7 presents nodes used to create two approximation polynomials and also the division of the domain into zones for which different polynomials have to be applied.

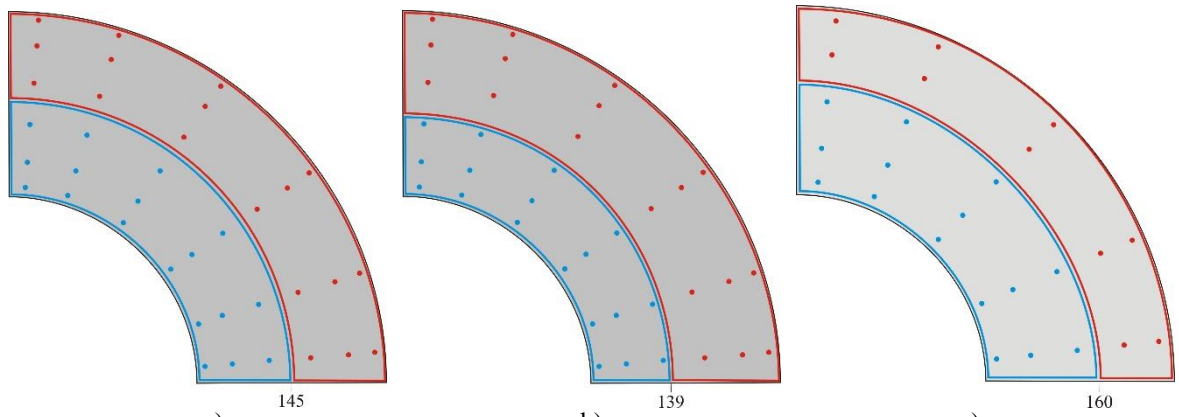

Figure 7: Different approaches for zonally local approximation

Figure 7a present arrangement of 36 interpolation nodes, which are divided into two groups for two approximation polynomials. In both of polynomials $T_1 = 3$ and $T_2 = 6$. Values of plastic strains at points from the zone with outer face with $r = 145$ are calculated using the first polynomial, while the rest using the second one. In the case presented in Fig. 7b the first zone of influence is reduced to favor the other ($r = 139$). This test is to check whether the maximum reduction of the zone with non-zero plastic strains affects the final results. The last from presented cases concerns approximation with 25 nodes. The first polynomial has $T_1 = 3$ and $T_2 = 5$, while the second $T_1 = 2$ and $T_2 = 5$. Zones of influence of individual polynomials are defined by the radius $r = 160$.

For the individual cases described above, the value of norm (14) has been determined. The results are presented in Table 2.

Table 2: Norms for radial and circumferential stress distribution – local approximation

	25,r=160	**36, r=145**	**36,r=139**
$\|e\|_{\sigma_r}$	0.3235	0.1561	0.1613

$\|e\|_{\sigma_\varphi}$	1.5861	1.0146	0.9195

Comparing the results presented in Tables 1 and 2, the following conclusions can be drawn:

a) the norm for radial stress reduces its value by 27%, while for circumferential stress by 35% when dividing into two polynomials and using totally 25 interpolation nodes,

b) for 36 nodes and the boundary between zones in $r = 145$ norms are reduced by 19% and 30% respectively for radial and circumferential stress (comparing to the global approach),

c) moving the boundary to $r = 139$ only affects the improvement of the norm for circumferential stress (in comparison to values obtained for $r = 145$).

As can be seen, there is an improvement in the results after dividing the domain into two approximating zones. Another important benefit is the shortening of calculation time. Thus, the calculations for 25 interpolation node divided into two polynomials is about 2.5 times shorter than for the global case. Taking into account the 36 interpolation nodes, the time is even shorter by 3.5 times.

5.2 Inverse distance weighting

Second example concerns the cantilever beam presented in Fig. 8. The beam is end-loaded and is considered as plane stress. The material parameters for this example are: $E = 2*10^{11} Pa$ and $v = 0.25$. The Von Mises yield criterion is assumed to apply with $\sigma_Y = 20 Pa$ and $H' = 0$.

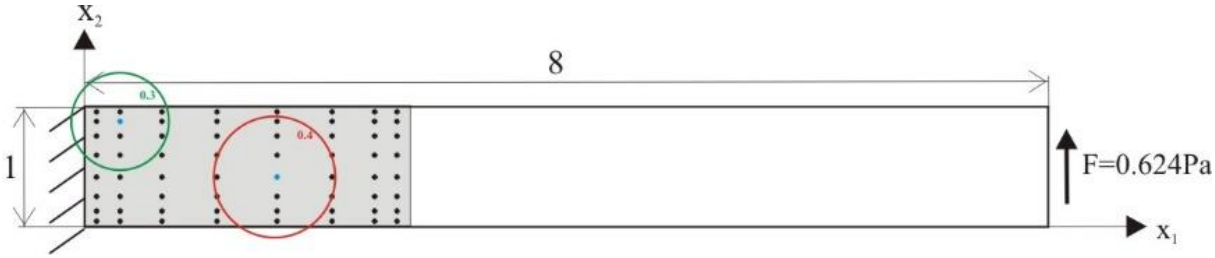

Figure 8: The considered cantilever beam

In the proposed method, like in BEM, only the plastic region is modeled. The considered example is described by the analytical solution, therefore the spread of that region is known a priori. Thus, not the whole domain must be defined, only its part presented in Fig. 8 (filled with gray). This requires only one Bézier bilinear surface with four corner points.

In [17] analytical formulas for elastic-plastic boundary and tip deflection are presented. In order to obtain those quantities using PIES 64 interpolation nodes are placed at roots of Chebyshev polynomials. Two methods of approximation are applied: the global approximation using Lagrange polynomial and IDW method. The power parameter is assumed as $p = 2$, while the radius of the neighborhood of influence are 0.3 and 0.4 (they are marked in Fig. 8 by green and red circles respectively). Of course it should be remembered that both radii are defined in the basic unit area. Obtained force-deflection values are presented in Fig. 9.

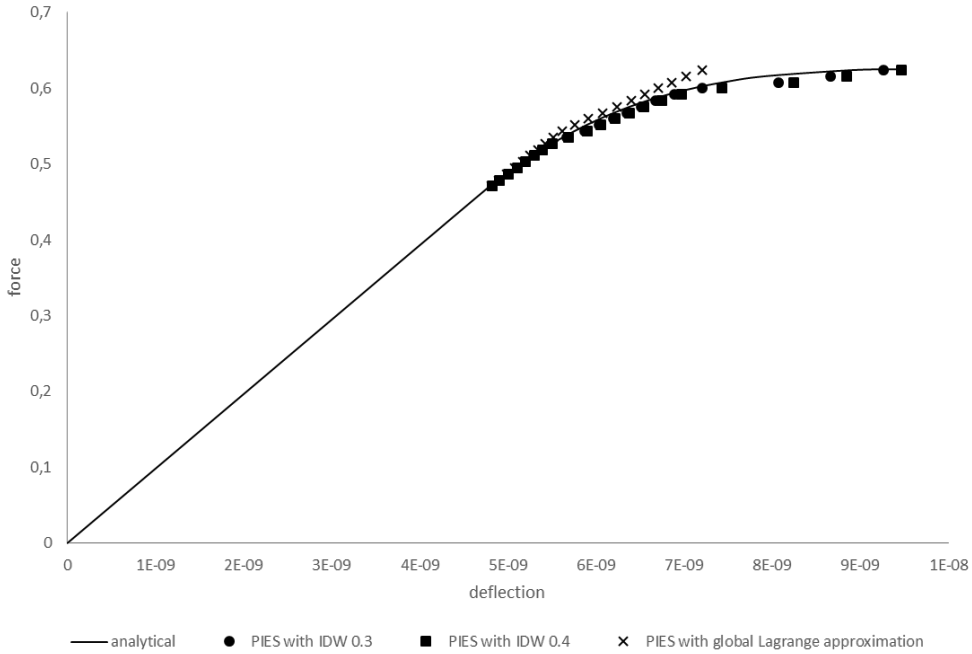

Figure 9: Force-deflection values for the cantilever beam

As can be seen in Fig. 9 solutions obtained by IDW with larger radius of neighborhood are slightly more accurate than those with a smaller radius. Both of them are more closer to analytical than those generated using global approximation with Lagrange polynomial. The latter reflect those obtained by FEM in [17].

Taking into account that slightly better results are obtained using larger radius of neighborhood in IDW method, the elastic-plastic boundary is determined using only this configuration. The boundary of the plastic zone determined analytically in comparison to plastified points obtained by PIES is presented in Fig. 10.

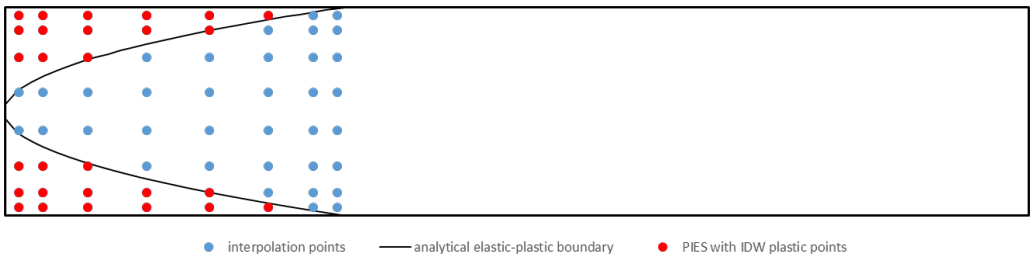

Figure 10: Comparison of plastic zones obtained by various method of approximation

As presented in Fig. 10, the spread of the plastic zone obtained by PIES with IDW method overlaps with analytical results. Having in mind also values of deflection shown above, it can be stated that the local approximation used in PIES method is very promising alternative to global approximation by various polynomials (e.g. Lagrange like in this paper).

6 CONCLUSIONS

The paper presents various methods of approximation of plastic strains in PIES. The PIES method is characterized by the global modeling of the plastic region, what gives the flexibility in application different approaches to approximation of solutions. Therefore, in the paper global and two local methods of approximation have been used. The first is zonally local, while the second takes into account only the influence of neighboring nodes.

Two examples were solved and results obtained were compared with analytical solutions. Moreover, numerical results obtained in the global manner are compared with the local one using different parameters.

It can be stated that using more than one approximation polynomial zonally is beneficial, because solutions obtained are more accurate. There was an improvement in accuracy up to 35%. Moreover, the time of calculations has decreased significantly (up to 3.5 times). Considering the IDW method applied to cantilever beam it is also shown that solutions obtained by local approach are more accurate than those received using global approximation.

REFERENCES

[1] Zienkiewicz, O.C. *The Finite Element Methods*. McGraw-Hill, (1977).

[2] Ameen, M. *Computational elasticity*. Alpha Science International Ltd., (2005).

[3] Aliabadi, M.H. *The boundary element method. Vol. 2. Applications in Solids and Structures*. John Wiley & Sons Ltd., (2002).

[4] Becker, A.A. *The boundary element method in engineering. A complete course*. McGraw-Hill, (1992).

[5] Zieniuk, E. Potential problems with polygonal boundaries by a BEM with parametric linear functions. *Engineering Analysis with Boundary Elements* (2001) **25(3)**: 185-190.

[6] Zieniuk, E. and Bołtuć, A. Bézier curves in the modeling of boundary geometry for 2D boundary problems defined by Helmholtz equation. *Journal of Computational Acoustics* (2006) **14(3)**: 353-367.

[7] Zieniuk, E. and Bołtuć, A. Non-element method of solving 2D boundary problems defined on polygonal domains modeled by Navier equation. *International Journal of Solids and Structures* (2006) **43(25-26)**: 7939-7958.

[8] Boltuc, A. and Zieniuk, E. Numerical approximation strategy for solutions and their derivatives for two-dimensional solids. *Applied Mathematical Modelling* (2015) **39(18)**: 5370-5391.

[9] Boltuc, A. Parametric integral equation system (PIES) for 2D elastoplastic analysis. *Engineering Analysis With Boundary Elements* (2016) **69**: 21-31.

[10] Farin, G. *Curves and surfaces for CAGD: A practical Guide*. Morgan Kaufmann Publishers, (2002).

[11] Salomon, D. *Curves and Surfaces for Computer Graphics*. Springer, (2006).

[12] Beer, G. and Smith, I. and Duenser, C. *The Boundary Element Method with Programming. For Engineers and Scientists*. Springer-Verlag Wien, (2008).

[13] Gao, X.W. Evaluation of regular and singular domain integrals with boundary-only discretization – theory and Fortran code. *Journal of Computational and Applied Mathematics* (2005) **175**: 265-290.

[14] Shepard, D. A two-dimensional interpolation function for irregularly-spaced data. Proceedings of the 1968 ACM National Conference (1968) 517–524, doi:10.1145/800186.810616.
[15] Liu, G.R. *Meshfree Methods: Moving Beyond the Finite Element Method*. CRC Press, (2009).
[16] Prager, R.M. and Hodge, P.G. *Theory of Perfectly Plastic Solids*. Dover Publications, (1951).
[17] Lubliner, J. *Plasticity theory*. Macmillan Publishing Company, (1990).